

Occupation Statistics of a Bose-Einstein Condensate for a Driven Landau-Zener Crossing

Katrina Smith-Mannschott,^{1,2} Maya Chuchem,³ Moritz Hiller,⁴ Tsampikos Kottos,¹ and Doron Cohen³

¹*Department of Physics, Wesleyan University, Middletown, Connecticut 06459, USA*

²*MPI for Dynamics and Self-Organization, Bunsenstr a e 10, D-37073 G ottingen, Germany*

³*Department of Physics, Ben-Gurion University, Beer-Sheva 84105, Israel*

⁴*Physikalisches Institut, Albert-Ludwigs-Universit at, Hermann-Herder-Stra e 3, D-79104 Freiburg, Germany*

(Received 19 January 2009; published 8 June 2009)

We consider an atomic Bose-Einstein condensate loaded in a biased double-well trap with tunneling rate K and interatomic interaction U . The Bose-Einstein condensate is prepared such that all N atoms are in the left well. We drive the system by sweeping the potential difference \mathcal{E} between the two wells. Depending on the interaction $u = NU/K$ and the sweep rate $\dot{\mathcal{E}}$, we distinguish three dynamical regimes: *adiabatic*, *diabatic*, and *sudden* and consider the occupation statistics of the final state. The analysis goes beyond mean-field theory and is complemented by a semiclassical picture.

DOI: 10.1103/PhysRevLett.102.230401

PACS numbers: 03.75.Lm, 03.65.-w, 05.30.Jp, 34.10.+x

The theoretical and experimental study of driven atomic Bose-Einstein condensates (BECs) in a few-site system using optical lattice technology has intensified in recent years [1–4]. Beyond the fundamental interest of these studies, they also aim to create a new generation of nano-scale devices such as atom transistors [5]. Consequently, a wealth of research has been done on the prototype two-site (dimer) system, either within the framework of a nonlinear mean-field approach [1], optionally using higher order cumulants [6], or adopting a conventional many-body perspective [7–10]. Such investigations have revealed many interesting phenomena associated with eigenvalue spectra, the structure of the eigenstates, wave-packet dynamics, e.g., of the Bloch-Josephson type, and leaking dynamics due to dissipative edges.

Driven dimers prove to be even more challenging [11–15]. The scenario investigated in these studies involves many-body Landau-Zener (LZ) transitions induced by sweeping the potential difference \mathcal{E} between the two wells. Specifically, one assumes that initially \mathcal{E} is very negative and that all $n = N$ atoms are in the first well. Then \mathcal{E} is increased at some constant rate $\dot{\mathcal{E}}$ to a very positive value. The objective is to calculate how many atoms (n) remain in the first well. The majority of published works are based on the Gross-Pitaevskii equation (or its discrete analogue), which is a mean-field approach [11,12]. There are only a few studies that have made further progress within the framework of a full quantum mechanical treatment of the system [13–15]. However, they all focus on calculating the average occupation $\langle n \rangle$, neglecting to form a theory for the occupation statistics $P(n)$ and, in particular, for the variance $\text{Var}(n)$.

Outline.—In this Letter, we consider a driven dimer with intersite hopping amplitude K and interatomic interaction U . The parameter $u = NU/K$ can be either positive (repulsive) or negative (attractive), and its magnitude determines various dynamical regimes [16]: Rabi ($|u| < 1$), Josephson ($1 < |u| < N^2$), or Fock ($|u| > N^2$). Depend-

ing on the sweep rate $\dot{\mathcal{E}}$, we distinguish between *adiabatic*, *diabatic*, and *sudden* dynamical scenarios and study the asymptotic occupation statistics as a function of u . Our analysis goes beyond mean-field theory, using a semiclassical picture and involving detailed simulations.

Modeling.—The simplest model that describes interacting bosons on a lattice is the Bose-Hubbard Hamiltonian (BHH), which in the case of the dimer (two sites) reads

$$\mathcal{H} = \sum_{i=1}^2 \left[\mathcal{E}_i \hat{n}_i + \frac{U}{2} \hat{n}_i (\hat{n}_i - 1) \right] - \frac{K}{2} \sum_{i \neq j} \hat{b}_i^\dagger \hat{b}_j, \quad (1)$$

with $\hbar = 1$, where \hat{b}_i and \hat{b}_i^\dagger are bosonic annihilation and creation operators, respectively, and $\hat{n}_i = \hat{b}_i^\dagger \hat{b}_i$ counts the number of particles at site $i = 1, 2$. The validity of this two-mode approximation [17] for a double well is discussed in Refs. [18,19], as well as in Ref. [20] for biased systems, and it was found to yield good agreement with the experiment [16]. The total number of particles $N = \hat{n}_1 + \hat{n}_2$ is a constant of motion, allowing us to consider a Hilbert space of dimension $\mathcal{N} = N + 1$, which is spanned by the Fock basis states $|n\rangle \equiv |n_1 = n, n_2 = N - n\rangle$. Below, we assume an even $N \gg 1$ and define $j = N/2$; hence $\mathcal{N} = 2j + 1$. The BHH for a given N is formally equivalent to the Hamiltonian of a spin j particle. By defining $J_z \equiv (\hat{n}_1 - \hat{n}_2)/2$ and $J_+ \equiv \hat{b}_1^\dagger \hat{b}_2$, it can be rewritten as

$$\hat{H} = U \hat{J}_z^2 + \mathcal{E} \hat{J}_z - K \hat{J}_x; \quad \mathcal{E} = \mathcal{E}_1 - \mathcal{E}_2, \quad (2)$$

where \mathcal{E} is the bias. In the absence of interaction, this Hamiltonian can be reinterpreted as describing a spin in a magnetic field with precession frequency $\Omega = (-K, 0, \mathcal{E})$.

The many-body Landau-Zener scenario assumes that initially all particles are located in the first site $|\Psi(t=0)\rangle = |N\rangle$. The bias \mathcal{E} is then varied with some constant sweep rate $\dot{\mathcal{E}}$. At the end of the sweep, the occupation statistics $P(n) \equiv |\langle n | \Psi(t) \rangle|^2$ becomes time-independent. Depending on the outcome (Fig. 1) we dis-

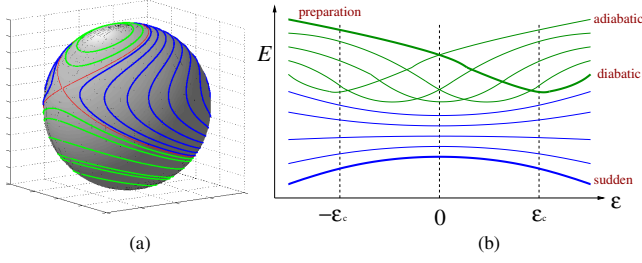


FIG. 1 (color online). Phase space and corresponding energy levels (conceptual plot). Note that a ground state preparation of a $U < 0$ system with increasing bias $\mathcal{E}(t)$ is equivalent to a preparation in the most excited state of a $U > 0$ system with decreasing bias. The latter convention has been adopted in the right panel and in our simulations.

tinguish among (i) an adiabatic process $P(n) \approx \delta_{n,0}$, (ii) a sudden process $P(n) \approx \delta_{n,N}$, and (iii) a diabatic process $P(n) \approx \delta_{n,n_c}$, where $n_c \neq 0, N$.

Phase space.—In order to analyze the dynamics for finite U , it is convenient to rewrite the BHH using canonical variables. Formally, our system corresponds to two coupled oscillators, and thus we can define action-angle variables $\hat{b}_i \equiv \sqrt{\hat{n}_i} \exp(i\varphi_i)$. Note that the translationlike operator $\exp(i\varphi)$ is in fact nonunitary because it annihilates the ground state, but this is irrelevant for $N \gg 1$ [16,21]. With these coordinates the BHH takes a form that resembles the Josephson Hamiltonian:

$$\mathcal{H} \approx \frac{NK}{2} \left[\frac{1}{2} u (\cos\theta)^2 + \epsilon \cos\theta - \sin\theta \cos\varphi \right], \quad (3)$$

where θ is an alternative way to express the occupation difference $J_z \equiv (\hat{n}_1 - \hat{n}_2)/2 \equiv (N/2) \cos(\theta)$ and $\varphi \equiv \varphi_1 - \varphi_2$. The scaled bias is $\epsilon \equiv \mathcal{E}/K$. Note that φ and θ do not commute. The classical phase space is described either using the canonical coordinates (φ, n) , with $n \equiv J_z + (N/2) \in [0, N]$, or equivalently using the spherical coordinates (φ, θ) . In the former case the total area of phase space is $2\pi N$ with a Planck cell $2\pi\hbar$ and $\hbar = 1$, while in the latter case the phase space has total area 4π with a Planck cell $4\pi/N$. Within the semiclassical approximation, a quantum state is described as a distribution in phase space and the eigenstates are associated with stripes that are stretched along contour lines $\mathcal{H}(\varphi, \theta) = E$. The energy levels E_n can be determined via WKB quantization of the enclosed phase space area.

Separatrix.—The phase space topology becomes non-trivial, i.e., has more than one component as in Fig. 1(a), if $|u| > 1$ and $|\epsilon| < \epsilon_c$ where $\epsilon_c = (u^{2/3} - 1)^{3/2}$. In this regime, a separatrix divides the phase space into three regions: two *islands* (green) that contain the upper energy levels and a *sea* (blue) that contains the lower energy levels. In this description and in the numerics below, we assume $U > 0$ and adopt the following enumeration convention: We define E_0 as the most excited level, while E_N

corresponds to the lowest one. Note that the replacement $U \mapsto -U$ would merely invert the order of the levels, and E_0 would become the ground state.

Figure 1(b) is an illustration of the energy levels as a function of the bias. Each level is associated via WKB quantization with one of the contour lines in Fig. 1(a). For the sake of our later analysis, we define E_{n_c} as the level which is closest to the separatrix for $|\epsilon| = \epsilon_c$. At this critical value of the bias, one of the islands has a vanishing phase space area, while the area of the other is $A_c \approx 4\pi\epsilon_c/u$. Using WKB quantization we get

$$n_c = \frac{A_c}{4\pi/N} \approx (1 - u^{-2/3})^{3/2} N, \quad (4)$$

where the approximation for A_c has been derived using methods as in Ref. [11] and has been tested numerically.

Simulations.—As a preliminary step, we did simulations of the undriven wave-packet dynamics with $\mathcal{E} = 0$ and $u = 2$. For this value of u , the separatrix crosses the north pole of the phase space, and therefore the wave packet stretches along it, as illustrated in Fig. 2(a) (classical) and in Fig. 2(b) (quantum mechanical). We note that this type of dynamics cannot be properly addressed by the mean-field approximation. The mean-field equation merely describes the Hamiltonian evolution of a single *point* in phase space and therefore assumes that the wave packet looks like a minimal Gaussian at any moment. Whenever the motion takes place near the separatrix, the mean-field description becomes inapplicable, and consequently the distribution $P(n)$ is likely *not* to be binomial [Fig. 2(c)]. In what follows, we use the terms sub-binomial (superbinomial) in order to refer to a $P(n)$ with a smaller (larger) spreading than the mean-field results. For the dynamics described in

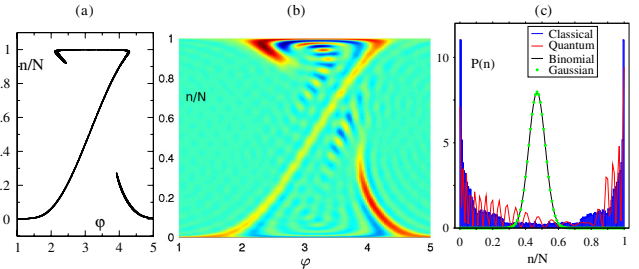


FIG. 2 (color online). Dynamical evolution in a situation in which the mean-field (Gaussian) approximation does not hold: $N = 100$ particles are prepared in one site of a symmetric ($\mathcal{E} = 0$) double well and then evolved with a $u = 2$ Hamiltonian. The initial wave packet is stretched along the separatrix. (a) (Semi) classical distribution in phase space. (b) Wigner function of the corresponding quantum state. (c) Quantum $P(n)$ compared with the (semi)classical and with the mean-field (binomial or Gaussian) predictions. The average occupation $\langle n \rangle = 47$ is associated here with a huge superbinomial variance $\text{Var}(n) = 1530$ instead of the binomial value $\text{Var}(n) \sim 25$. In all of the simulations, we use a 4th order Runge-Kutta and made sure that during the integration the probability leakage is $\ll 10^{-6}$.

Fig. 2, the stretching along the separatrix leads to a superbinomial result.

Next, we address the effect of separatrix motion on $P(n)$ in the bias-sweep scenario. Note that this separatrix motion cannot be avoided: For $\varepsilon < -\varepsilon_c$, the wave packet is localized in the upper level. When $\varepsilon = -\varepsilon_c$, the separatrix emerges. As long as $-\varepsilon_c < \varepsilon < 0$, the wave packet remains trapped in the top of the big island which gradually shrinks. When ε becomes larger than zero, the wave packet can partially tunnel out from the shrinking island to the levels of the expanding island. When $\varepsilon = +\varepsilon_c$, the shrinking island disappears, and the remaining part of the wave packet is squeezed out along the $n = n_c$ contour, resembling the dynamics of Fig. 2. One observes that the stretching along the separatrix during the nonlinear LZ transition is accompanied by narrowing in the transverse direction. This leads to a sub-binomial rather than superbinomial result for the distribution $P(n)$ at the end of the sweep.

In Fig. 3, we plot the average occupation $\langle n \rangle$ and the participation number $PN \equiv [\sum_n P(n)^2]^{-1}$ of the distribution at the end of the sweep as a function of $\dot{\varepsilon}$. These, unlike $\langle n \rangle$, provide significantly more information regarding the nature of the crossing process. For very slow rates, the wave packet follows a strict adiabatic process ending in $n = 0$; i.e., all particles move to the other site. For a moderate sweep rate, the wave packet ends in a superposition of $n = 0$ and $n = 1$ states, indicated by $PN = 2$. We also resolve the possibility of ending entirely at $n = 1$, at $n = 2$, or at $n = 3$. In the case shown in Fig. 3, we have $n_c \approx 4$. For larger sweep rates, we observe a qualitatively different behavior that can be described as a crossover from an adiabatic/diabatic behavior to a sudden behavior at the peak value $PN = 4$. In order to appreciate the deviation of

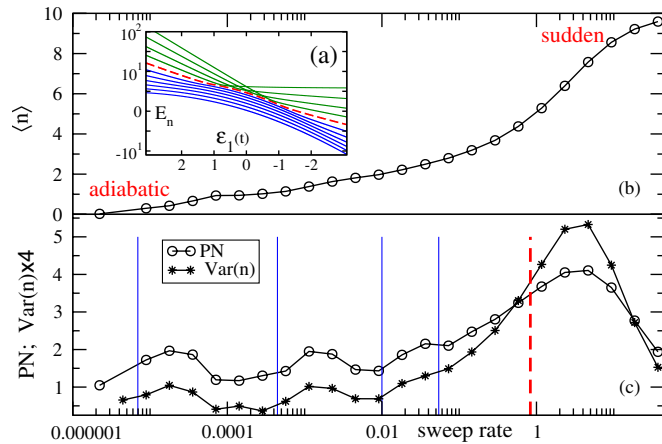


FIG. 3 (color online). (a) Parametric evolution of the adiabatic energy levels versus the decreasing $\mathcal{E}_1(t)$ for $N = 10$ particles and $u = 2.5$. We use units of time such that $K = 1$. The dashed line corresponds to the level $n_c = 4$. (b) Average occupation $\langle n \rangle$ versus the sweep rate $\dot{\varepsilon}$. (c) PN and $\text{Var}(n)$ versus $\dot{\varepsilon}$. The vertical lines indicate the various adiabatic and diabatic (dashed) thresholds.

the numerical results from the mean-field theory prediction, we plot $\text{Var}(n)$ versus $\langle n \rangle$ in Fig. 4 and compare with the binomial expectation. We further analyze the observed results in the last section.

Thresholds.—The various thresholds that are involved in the adiabatic-diabatic-sudden crossovers are indicated in Fig. 5. They all follow from the breakdown of a “slowness condition” that can be written as

$$\dot{\varepsilon} \ll \omega_{\text{osc}}^2 / \kappa, \quad (5)$$

where ω_{osc} is a characteristic frequency of the unperturbed dynamics and κ is the coupling parameter that determines the rate of the driven transitions.

In the strict quantum adiabatic framework, ω_{osc} is simply the level spacing and κ is determined by the slopes of the intersecting levels. In order to determine the adiabatic thresholds in Fig. 3, we observe that for the intersection of the 0th level with the $(N - n)$ level the difference in slope is $\kappa = (N - n)$, because asymptotically $d(E_n - E_m)/d\varepsilon \sim (n - m)$. In the absence of interaction ($u \ll 1$), the level spacing is $\omega_{\text{osc}} = K$ and only nearby levels are coupled, leading to the standard Landau-Zener adiabaticity condition $\dot{\varepsilon} \ll K^2$. With strong interaction there is an N th order coupling between the $n = 0$ level and the $n = N$ level, which allows tunneling from the top of one island to the top of the other island (as illustrated in Fig. 1). An estimate for this coupling is $K_{\text{eff}} = [NK]/[2^{N-1}(N-1)!](K/U)^{N-1}$ [7]. Similar considerations can be applied to the bottom sea level leading to the distinction between mega, gradual, and sequential crossings (see Ref. [22]).

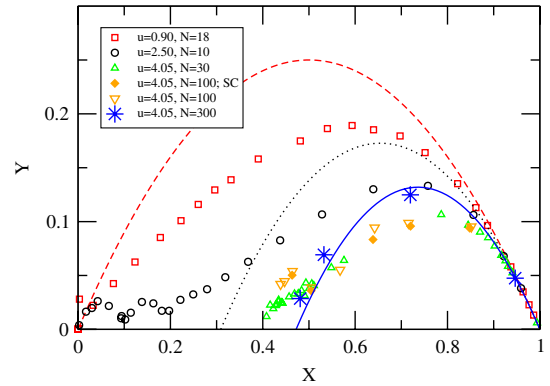


FIG. 4 (color online). $Y = \text{Var}(n)/N$ versus $X = \langle n \rangle/N$. Symbols correspond to numerical data, while lines indicate the sub-binomial scaling relation Eq. (6) with $u = 2.5$ (dotted line) and $u = 4.05$ (solid line). No fitting is involved. As a reference we plot the standard binomial scaling (dashed line) which would strictly apply in the absence of interaction ($u = 0$) and the results of semiclassical (SC) simulations which are obtained by running ensemble of trajectories in phase space. There is a clear crossover from a binomial to the sub-binomial scaling, and the agreement becomes better for large N . Note that the superbinomial data point $(X, Y) = (0.47, 15.3)$ that corresponds to the distribution in Fig. 2 is out-of-scale.

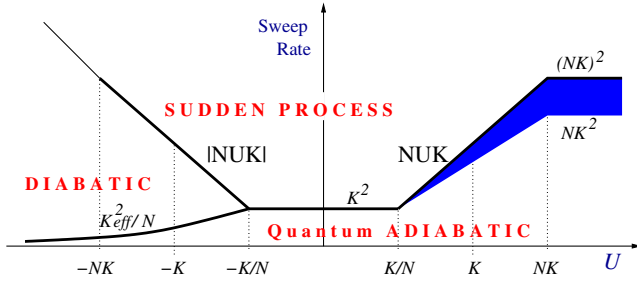


FIG. 5 (color online). Diagram of the $(U, \dot{\mathcal{E}})$ regimes for a ground state preparation. In the Rabi regime $|U| < K/N$, we have a crossover from adiabatic to sudden behavior. For $K/N < U < NK$ (or $U > NK$), we have a broad crossover from adiabatic gradual (or sequential [22]) behavior to sudden behavior. For $U < -K/N$, we have two crossovers: the first from quantum adiabatic to diabatic behavior and the second from diabatic to sudden behavior. The diabatic behavior can be regarded as a classical nonlinear adiabatic behavior. For $U < -NK$, the distinction between the diabatic and the sudden regime is blurred because the final state is the same.

For large N it might be practically impossible to satisfy the strict adiabatic condition which is associated with the possibility to tunnel from the top of one island to the top of the other. Then the relevant mechanism for transition, i.e., the emission to the level n_c as described in the previous section, becomes semiclassical. The frequency that governs this process is the oscillation frequency at the bottom of the sea $\omega_{\text{osc}} \sim |NUK|^{1/2}$. It determines the level spacing of the lower energy levels and also describes the level spacing in the vicinity of the separatrix, apart from some logarithmic corrections [23]. It follows that the diabatic-sudden crossover involves the threshold condition $\dot{\mathcal{E}} \ll |NUK|$ as indicated in Fig. 5 and in Fig. 3 for the specific parameters of the simulations.

Scaling.—Because of the squeezing along the separatrix, the spreading of the wave packet for an idealized diabatic process becomes negligible in the transverse direction. The diabatic-sudden crossover is related to the nonadiabatic transitions between the remaining $(N - n_c)$ sea levels, where nonlinear effects are negligible. It follows that the spreading can be approximately modeled by the toy Hamiltonian $\mathcal{H} = h(t) \cdot J$, where J is a spin entity with $j_{\text{eff}} = (N - n_c)/2$ and $h(t)$ is a field with constant magnitude $|h(t)| = \omega_{\text{osc}}$ corresponding to the mean-level spacing. The sweep is like a rotation of $h(t)$ in the plane with some angular rate ω . For such a (linear) model the mean-field approximation is exact, and therefore we suggest (due to the truncation of Hilbert space) a sub-binomial rather than binomial scaling relation between the mean and the variance of the occupation statistics:

$$Y = (1 - X) \frac{X - c}{1 - c}, \quad \text{with} \quad c = \frac{n_c}{N}, \quad (6)$$

where $X = \langle n \rangle / N$ and $Y = \text{Var}(N) / N$. Our numerical data

are reported in Fig. 4 together with the binomial ($c = 0$) and sub-binomial scaling relation Eq. (6). The numerics confirm the expected u -dependent crossover from binomial to sub-binomial statistics, where the latter, with no fitting parameters, sets a lower bound for the variance.

Summary.—In view of the strong research interest in counting statistics of electrons in mesoscopic devices, it is surprising that the issue of occupation statistics of BECs has been explored only for equilibrium phase transitions. We were motivated to address this subject in the framework of dynamical processes by state-of-the-art experiments aimed at counting individual particles [2–4]. We have shown that in the case of a many-body Landau-Zener transition the mean-field binomial expectation is not realized; however, a sub-binomial scaling relation still works quite well. The study of the occupation statistics and, in particular, the participation number of the final distribution allowed us to resolve all of the details of the adiabatic-diabatic-sudden crossovers and to verify theoretical estimates for the threshold of each crossover.

This research was funded by a grant from the U.S.–Israel Binational Science Foundation (BSF), the DFG Forschergruppe 760, and a DIP grant.

- [1] M. Albiez *et al.*, Phys. Rev. Lett. **95**, 010402 (2005).
- [2] C.S. Chuu *et al.*, Phys. Rev. Lett. **95**, 260403 (2005); A. M. Dudarev *et al.*, Phys. Rev. Lett. **98**, 063001 (2007).
- [3] S. Foelling *et al.*, Nature (London) **448**, 1029 (2007).
- [4] P. Cheinet *et al.*, arXiv:0804.3372.
- [5] J. A. Stickney *et al.*, Phys. Rev. A **75**, 013608 (2007).
- [6] J. R. Anglin and A. Vardi, Phys. Rev. A **64**, 013605 (2001); A. Vardi *et al.*, Phys. Rev. A **64**, 063611 (2001); Phys. Rev. Lett. **86**, 568 (2001).
- [7] G. Kalosakas *et al.*, Phys. Rev. A **68**, 023602 (2003); J. Phys. B **36**, 3233 (2003); Phys. Rev. A **65**, 043616 (2002).
- [8] F. Trimborn *et al.*, Phys. Rev. A **79**, 013608 (2009).
- [9] M. Hiller *et al.*, Phys. Rev. A **73**, 063625 (2006).
- [10] E. M. Graefe *et al.*, Phys. Rev. Lett. **101**, 150408 (2008).
- [11] J. Liu *et al.*, Phys. Rev. A **66**, 023404 (2002).
- [12] B. Wu and Q. Niu, Phys. Rev. A **61**, 023402 (2000).
- [13] D. Witthaut, E. M. Graefe, and H. J. Korsch, Phys. Rev. A **73**, 063609 (2006).
- [14] P. Solinas *et al.*, arXiv:0807.0703.
- [15] A. Atland and V. Gurarie, Phys. Rev. Lett. **100**, 063602 (2008).
- [16] R. Gati and M. K. Oberthaler, J. Phys. B **40**, R61 (2007).
- [17] G. J. Milburn *et al.*, Phys. Rev. A **55**, 4318 (1997).
- [18] R. W. Spekkens, J. E. Sipe, Phys. Rev. A **59**, 3868 (1999).
- [19] D. Ananikian and T. Bergeman, Phys. Rev. A **73**, 013604 (2006).
- [20] D. R. Dounas-Frazer *et al.*, Phys. Rev. Lett. **99**, 200402 (2007).
- [21] A. J. Leggett, Rev. Mod. Phys. **73**, 307 (2001).
- [22] M. Hiller *et al.*, Europhys. Lett. **82**, 40006 (2008); Phys. Rev. A **78**, 013602 (2008).
- [23] E. Boukobza *et al.*, Phys. Rev. Lett. **102**, 180403 (2009).